

## Supporting Information

### **Ruthenium supported on MIL-101 as an efficient catalyst for hydrogen generation from hydrolysis of amine boranes**

Nan Cao<sup>a</sup>, Teng Liu<sup>a</sup>, Jun Su<sup>c</sup>, Xiaojun Wu<sup>a</sup>, Wei Luo<sup>a,b\*</sup>, Gongzhen Cheng<sup>a</sup>

<sup>a</sup>College of Chemistry and Molecular Sciences, Wuhan University, Wuhan, Hubei 430072, P. R. China.

Tel.: +86 2768752366. *E-mail address*: wluo@whu.edu.cn

<sup>b</sup>Suzhou Institute of Wuhan University, Suzhou, Jiangsu, 215123, P. R. China

<sup>c</sup>Wuhan National Laboratory for Optoelectronics, Huazhong University of Science and Technology, Wuhan, Hubei, 430074, P. R. China

## **Experimental**

### **Chemicals and materials**

All chemicals were commercial and used without further purification. Chromic nitrate nonahydrate ( $\text{Cr}(\text{NO}_3)_3 \cdot 9\text{H}_2\text{O}$ , Sinopharm Chemical Reagent Co., Ltd., 99%), Ruthenium chloride hydrate ( $\text{RuCl}_3 \cdot n\text{H}_2\text{O}$ , Wuhan Greatwall Chemical Co., Ltd., 99%), methylamine hydrochloride ( $\text{CH}_3\text{NH}_2 \cdot \text{HCl}$ , Sinopharm Chemical Reagent Co., Ltd.,  $\geq 96\%$ ), ammonia borane ( $\text{NH}_3 \cdot \text{BH}_3$ , AB, Aldrich, 90%), aqueous hydrofluoric acid (HF, Sinopharm Chemical Reagent Co., Ltd., 40%), terephthalic acid ( $\text{HO}_2\text{CC}_6\text{H}_4\text{CO}_2\text{H}$ , Sinopharm Chemical Reagent Co., Ltd., 99%), sodium borohydride ( $\text{NaBH}_4$ , Sinopharm Chemical Reagent Co., Ltd., 96%), Ammonium fluoride ( $\text{NH}_4\text{F}$ , Sinopharm Chemical Reagent Co., Ltd.,  $\geq 96\%$ ), ethanol ( $\text{C}_2\text{H}_5\text{OH}$ , Sinopharm Chemical Reagent Co., Ltd.,  $>99.8\%$ ) were used as received. We use

ordinary distilled water as the reaction solvent.

### **Synthesis of MIL-101**

MIL-101 was synthesized using the reported procedure.<sup>S1</sup> Terephthalic acid (332 mg, 2.0 mmol),  $\text{Cr}(\text{NO}_3)_3 \cdot 9\text{H}_2\text{O}$  (800 mg, 2.0 mmol), aqueous HF (0.1 mL, 40 wt%) and de-ionized water (9.6 mL) were placed in a 50 mL Teflon-liner autoclave and heated at 220 °C for 8 h. After natural cooling, the suspension was centrifuged to separate the green powder of MIL-101 with formula  $\text{Cr}_3\text{F}(\text{H}_2\text{O})_2\text{O}[(\text{O}_2\text{C})\text{C}_6\text{H}_4(\text{CO}_2)]_3 \cdot n\text{H}_2\text{O}$  ( $n \approx 25$ ), and then further purified by solvothermal treatment in ethanol at 80 °C for 24 h. The resulting green solid was soaked in  $\text{NH}_4\text{F}$  (1 M) solution at 70 °C for 24 h to eliminate the terephthalic acid inside the pores of MIL-101 and immediately filtered resulting green solid was finally dried overnight at 150 °C under vacuum for further use.

### **Preparation of methyl ammonia borane( $\text{CH}_3\text{NH}_2\text{-BH}_3$ , MeAB)**

MeAB was synthesized by the method reported in the literature.<sup>S2</sup> Sodium borohydride (1.89g, 0.05mol) and methylamine hydrochloride (3.37 g, 0.05mol) were added to a 250 mL two-neck round-bottom flask with a neck connected to a condenser. THF (100 mL) was transferred into the flask, and the contents were vigorously stirring. The reaction was carried out at room temperature under nitrogen atmosphere. After 12 hs, the resultant solution was filtered by suction filtration and the filtrate was concentrated under vacuum at room temperature. After dissolved in 100 mL diethyl ether at 0 °C and stirred for 2 hs, MeAB was obtained by remove the solvent under vacuum.

### **Synthesis of Ru@MIL-101**

Activated MIL-101 (100 mg) was mixed with 10 mL de-ionized water containing

(0.01, 0.03, 0.04, 0.05, 0.07 mmol)  $\text{RuCl}_3$  and stirring was continued for 12 h at  $25^\circ\text{C}$  to impregnate metal salts, then reduced by sodium borohydride ( $\text{NaBH}_4$ , 75.6 mg) solution with vigorous stirring at  $0^\circ\text{C}$  to yield  $\text{Ru@MIL-101}$ . The physical mixture of Ru and MIL-101 performed in the similar way. The solution of equal amount  $\text{RuCl}_3$  reduced by sodium borohydride and then mixed with 50 mg MIL-101.

### **Hydrolytic dehydrogenation of ammonia borane and methyl ammonia borane**

A mixture of 50 mg  $\text{Ru@MIL-101}$  and 5 mL de-ionized water were kept in a two-necked round-bottom flask. One neck was connected to a pressure-equalization funnel to introduce 2 mL aqueous solution of  $\text{NH}_3\text{BH}_3$  (30.8 mg, 1 mmol) or  $\text{CH}_3\text{NH}_2\text{BH}_3$  (45 mg, 1 mmol), and the other neck was connected to a gas burette to monitor the volume of the gas evolution. The reactions were carried out at  $25^\circ\text{C}$  in air. Temperature was varied at  $25 \pm 0.2^\circ\text{C}$ ,  $30 \pm 0.2^\circ\text{C}$ ,  $35 \pm 0.2^\circ\text{C}$  and  $40 \pm 0.2^\circ\text{C}$  while the catalyst (50 mg) and AB (or MeAB, 1 mmol) were kept constant to obtain the activation energy ( $E_a$ ).

### **Stability test**

2 mL of solution containing 30.8 mg AB (or 45.0 mg MeAB) was added to 5 mL of water dissolved 50 mg  $\text{Ru@MIL-101}$ , the evolution of gas was monitored as described above. After the hydrogen generation reaction was completed, new aqueous AB solution (30.8 mg, 2 mL) or MeAB solution was added into the reaction flask. The evolution of gas was monitored using the gas burette. Such cycle tests of the catalyst for the hydrolysis of AB and MeAB were carried out five times in air.

## **2.7 Characterization**

The morphologies and sizes of the samples were observed by using a Tecnai G20 U-

Twin transmission electron microscope (TEM) equipped with an energy dispersive X-ray detector (EDX) at an acceleration voltage of 200 kV. Powder X-ray diffraction (XRD) patterns were measured by a Bruker D8-Advance X-ray diffractometer using Cu Ka radiation source ( $\lambda = 0.154178$  nm) with a velocity of  $1^\circ \text{ min}^{-1}$ . The surface area measurements were performed with N<sub>2</sub> adsorption/desorption isotherms at liquid nitrogen temperature (77 K) after dehydration under vacuum at 150 °C for 12 h using Quantachrome NOVA 4200e. The inductively coupled plasma-atomic emission spectroscopy (ICP-AES) was performed on IRIS Intrepid II XSP (Thermo Fisher Scientific, USA).

## References

- S1 G. Férey, C. Mellot-Draznieks, C. Serre, F. Millange, J. Dutour, S. Surblé and I. Margiolaki, *Science*, 2005, **309**, 2040.
- S2 Z. X. Yang, F. Y. Cheng, Z. L. Tao, J. Liang and J. Chen, *Int. J. Hydrogen Energy*, 2012, **37**, 7638.
- S3 H. Y. Liang, G. Z. Chen, S. Desinan, R. Rosei, F. Rosei and D. L. Ma, *Int. J. Hydrogen Energy*, 2012, **37**, 17921.
- S4 S. Akbayrak and S. Özkar, *ACS Appl. Mater. Interfaces*, 2012, **4**, 6302.
- S5 Ö. Metin, Ş. Şahin and S. Özkar, *Int. J. Hydrogen Energy*, 2009, **34**, 6304.
- S6 N. Cao, W. Luo and G. Z. Cheng, *Int. J. Hydrogen Energy*, 2013, **34**, 11964.
- S7 H. Can and Ö. Metin, *Appl. Catal. B*, 2012, **125**, 304.
- S8 M. Chandra and Q. Xu, *J. Power Sources*, 2007, **168**, 135.
- S9 F. Durap, M. Zahmakıran and S. Özkar, *Int. J. Hydrogen Energy*, 2009, **34**, 7223.

- S10 N. Cao, J. Su, W. Luo and G. Z. Cheng, *Catal. Commun.*, 2014, **43**, 47.
- S11 N. Cao, J. Su, W. Luo and G. Z. Cheng, *Int. J. Hydrogen Energy*, 2014, **39**, 426.
- S12 G. Z. Chen, S. Desinan, R. Nechache, R. Rosei, F. Rosei and D. L. Ma, *Chem. Commun.*, 2011, **47**, 6308.
- S13 N. Cao, J. Su, X. L. Hong, W. Luo and G. Z. Cheng, *Chem. Asian J.*, 2014, **9**, 562.
- S14 G. P. Rachiero, U. B. Demirci and P. Miele, *Catal. Today*, 2011, **170**, 85.
- S15 G. P. Rachiero, U. B. Demirci and P. Miele, *Int. J. Hydrogen Energy*, 2011, **36**, 7051.
- S16 N. Cao, K. Hu, W. Luo and G. Z. Cheng, *J. Alloy Compd.*, 2014, **590**, 241.

Table S1. Catalytic activity of Ru-based catalysts used for the hydrolytic dehydrogenation of AB

Catalyst	TOF(mol H <sub>2</sub> mol <sup>-1</sup> metal min <sup>-1</sup> )	Ea (kJ mol <sup>-1</sup> )	Ref.
Ru/C	429.5	34.81	S3
Ru(0)@MWCNT	329	33	S4
PSSA-co-MA stabilized Ru nanoclusters	187.6	54	S5
2.80 wt% Ru@MIL-101	178	--	This study
1.62 wt% Ru@MIL-101	147.6	51.12	This study
Ru/graphene	100	11.7	S6
Ru@Al <sub>2</sub> O <sub>3</sub> after acetic acid treatment	83.3	46	S7
Ru/ $\gamma$ -Al <sub>2</sub> O <sub>3</sub> laurate-stabilized ruthenium(0) nanoclusters	77	23	S8
	75	47	S9
Ru@Co/graphene	40.5	--	S10
Ru@Ni/graphene	39.9	36.6	S11
Ru@Al <sub>2</sub> O <sub>3</sub>	39.6	48	S7
Ni@Ru	30.6	44	S12
Ru@Ni/C black	29.4	37.9	S13
Ru@Co/C black	29.1	21.2	S13
Ru/ $\gamma$ -Al <sub>2</sub> O <sub>3</sub>	23.05	67	S14
RuCo (1:1)/ $\gamma$ -Al <sub>2</sub> O <sub>3</sub>	16.5	47	S15
RuCu/graphene	15.9	30.4	S16
RuCu (1:1)/ $\gamma$ -Al <sub>2</sub> O <sub>3</sub>	8.2	52	S15

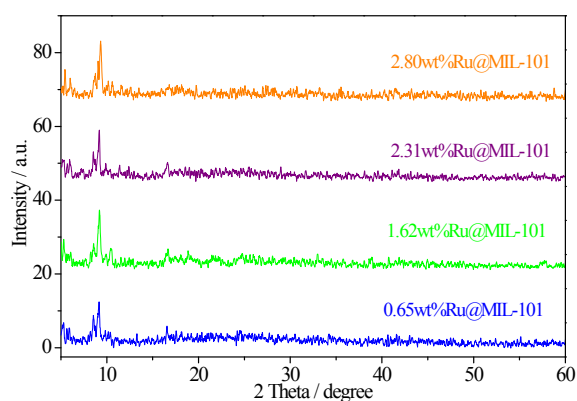


Figure S1 The wide-angle PXRD patterns of samples.

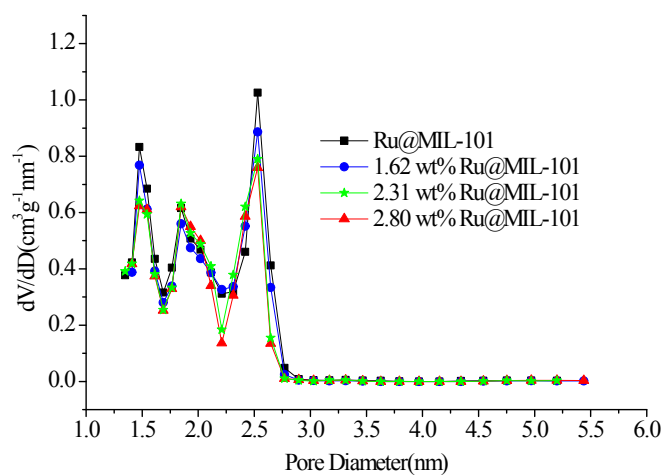


Figure S2 The pore diameter distribution of MIL-101 and Ru@MIL-101.

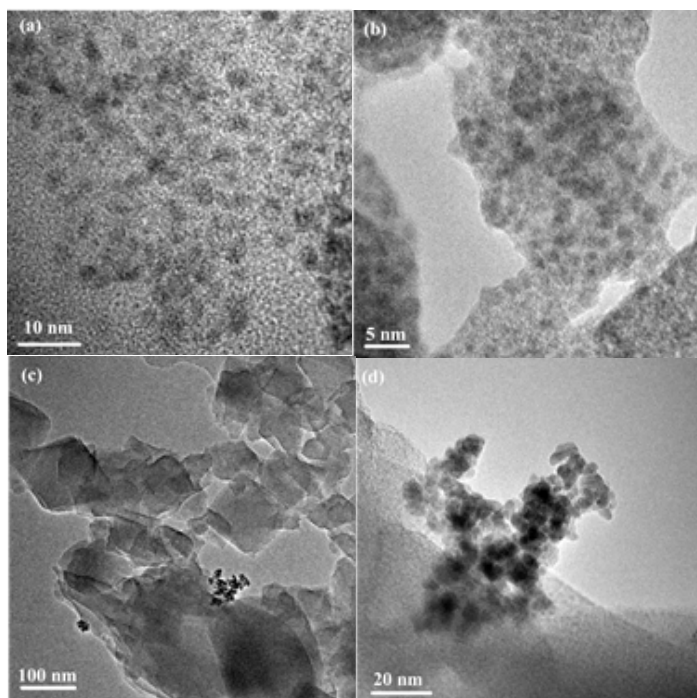


Figure S3. (a-b) TEM images of 2.31 wt% Ru@MIL-101; (c-d) TEM images of a physical mixture of Ru NPs and MIL-101.

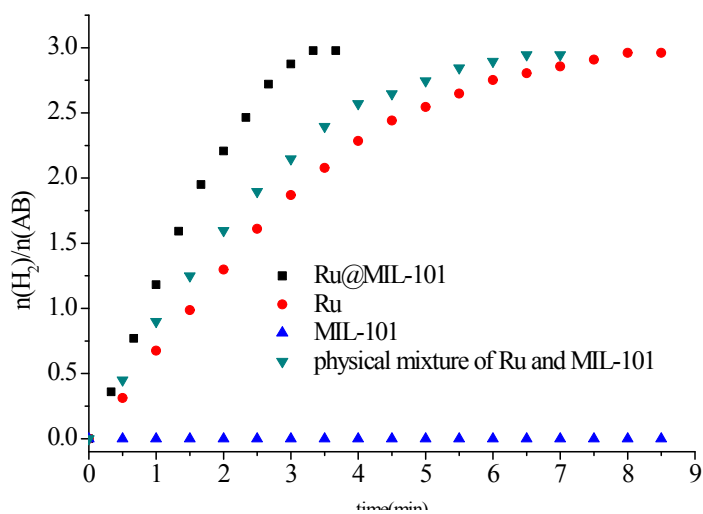


Figure S4. Time plots of catalytic dehydrogenation of AB by Ru, MIL-101, Ru@MIL-101 and a physical mixture of Ru NPs and MIL-101. (Ru/AB = 0.008)

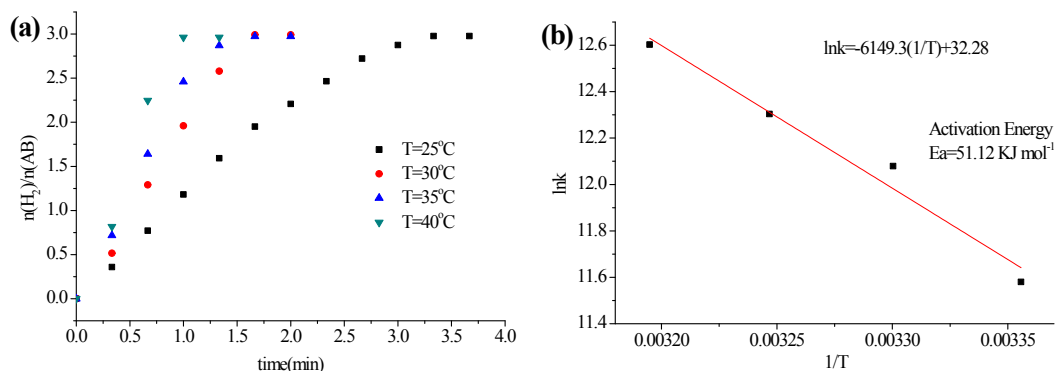


Figure S5. (a) Time course plots for hydrogen generation by the decomposition of AB by 1.62 wt% Ru@MIL-101 at different temperatures. (b) Plot of  $\ln k$  versus  $1/T$  during the AB decomposition over 1.62 wt% Ru@MIL-101 at different temperatures.



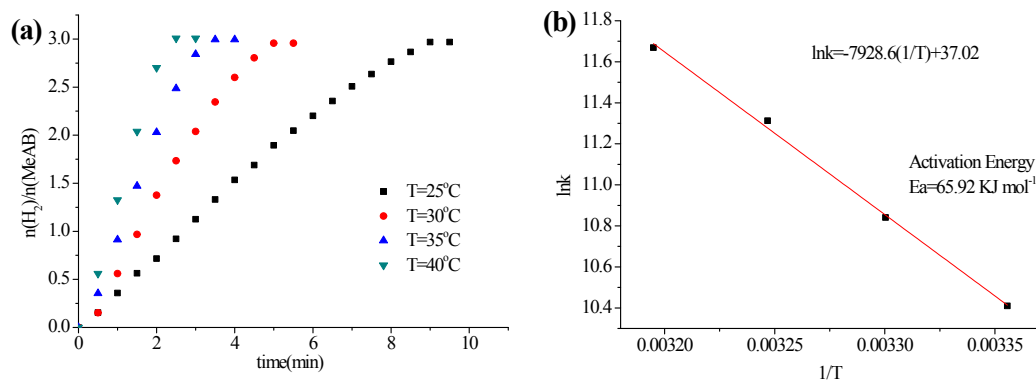


Figure S6. (a) Time course plots for hydrogen generation by the decomposition of MeAB by 1.62 wt% Ru@MIL-101 at different temperatures. (b) Plot of  $\ln k$  versus  $1/T$  during the MeAB decomposition over 1.62 wt% Ru@MIL-101 at different temperatures .

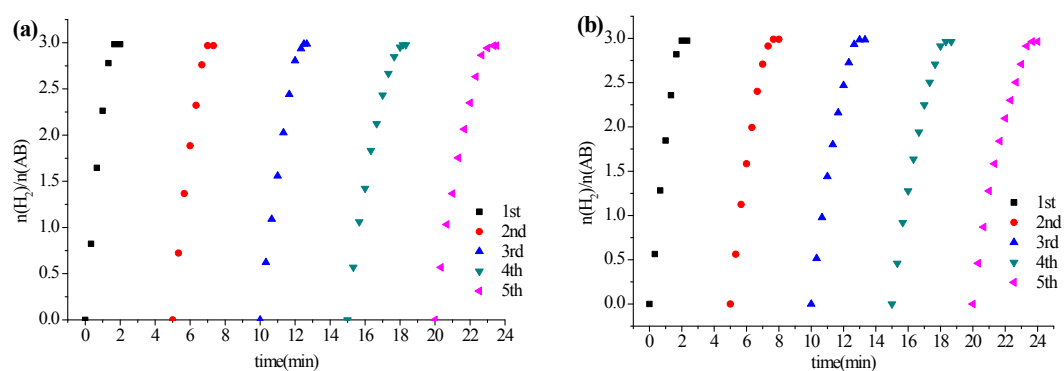


Figure S7. Durability test of (a) 2.31 wt% Ru@MIL-101 and (b) 2.80 wt% Ru@MIL-101 for decomposition of AB.